ROS are evolutionary conserved cell-to-cell stress signals

Yosef Fichman[a] (ID), Linda Rowland[b] (ID), Melvin J. Oliver[a] (ID), and Ron Mittler[a,b,1] (ID)

Cell-to-cell communication is fundamental to multicellular organisms and unicellular organisms living in a microbiome. It is thought to have evolved as a stress- or quorum-sensing mechanism in unicellular organisms. A unique cell-to-cell communication mechanism that uses reactive oxygen species (ROS) as a signal (termed the "ROS wave") was identified in flowering plants. This process is essential for systemic signaling and plant acclimation to stress and can spread from a small group of cells to the entire plant within minutes. Whether a similar signaling process is found in other organisms is however unknown. Here, we report that the ROS wave can be found in unicellular algae, amoeba, ferns, mosses, mammalian cells, and isolated hearts. We further show that this process can be triggered in unicellular and multicellular organisms by a local stress or H_2O_2 treatment and blocked by the application of catalase or NADPH oxidase inhibitors and that in unicellular algae it communicates important stress–response signals between cells. Taken together, our findings suggest that an active process of cell-to-cell ROS signaling, like the ROS wave, evolved before unicellular and multicellular organisms diverged. This mechanism could have communicated an environmental stress signal between cells and coordinated the acclimation response of many different cells living in a community. The finding of a signaling process, like the ROS wave, in mammalian cells further contributes to our understanding of different diseases and could impact the development of drugs that target for example cancer or heart disease.

reactive oxygen species | hydrogen peroxide | evolution | signal transduction | ROS wave

Cells communicate with each other in many ways. The exchange of signals between cells is thought to have evolved as part of a mechanism to control cell density (e.g., quorum sensing; refs. 1 and 2) and/or as part of a response mechanism to changes in environmental conditions (e.g., in cells living in a biofilm; refs. 3 and 4). Cell-to-cell communication can occur between cells of the same species or organism (e.g., in a multicellular organism; refs. 5 and 6), as well as between cells of different organisms (e.g., during interactions of cells with different bacterial or fungal pathogens; refs. 7 and 8). Two of the most conserved cell-to-cell signaling pathways are paracrine, secretion of signals that are perceived by neighboring cells, and juxtacrine, communication between cells connected via tunneling nanotubes, gap junctions, or plasmodesmata (PD; refs. 9–12). With the evolution of the vascular and nervous systems, paracrine signaling was extended to endocrine signaling, the release of signals into the bloodstream, and paracrine and juxtacrine signaling began to contribute to long-distance signaling as part of electrical and chemical synapses (5, 6). In addition, autocrine signaling evolved as a mechanism for cells to regulate their own function (13). Cell-to-cell signaling therefore plays a pivotal role in coordinating the developmental and environmental responses of groups of neighboring cells as well as cells that are remotely connected via blood vessels or neurons.

In vascular plants, that lack true nervous and circulatory systems, local cell-to-cell communication is primarily mediated by paracrine (via the apoplast) and juxtacrine (via PD) signaling, while long-distance signaling is mediated through the vascular system (14, 15). Among the key signals exchanged by plant cells are different metabolites, small RNA and peptide molecules, hormones, calcium, volatile compounds, hydraulic pressure signals, electric signals, and reactive oxygen species (ROS), such as hydrogen peroxide (H_2O_2; refs. 14–18). A unique and rapid cell-to-cell signaling mechanism discovered in flowering plants is the "ROS wave" (19–21). The ROS wave is an autopropagating cell-to-cell signaling pathway in which the initiating cell activates extracellular (apoplastic) superoxide ($O_2^{.-}$) production via respiratory burst oxidase homologs [RBOHs; the plant homologs of NADPH oxidases (NOXs); refs. 19–21]. The $O_2^{.-}$ produced by this cell rapidly dismutates into H_2O_2 that is sensed by neighboring cells and triggers in them a similar enhanced $O_2^{.-}/H_2O_2$ production process, resulting in the activation of a cascade or wave of cell-to-cell "enhanced $O_2^{.-}/H_2O_2$ production state" that spreads from the initiating cells/tissues over long distances, sometimes spanning the entire length of the plant (20, 21). In addition to spreading from cell-to-cell within a plant, the ROS wave was recently shown to spread

Significance

Reactive oxygen species (ROS) play a pivotal role in the regulation of cell metabolism, development, and responses to the environment. In flowering plants, reactive oxygen species were found to play a cell-to-cell signaling role mediating systemic long-distance responses to different stimuli (termed the "ROS wave"). Here, we reveal that ROS mediate a similar process of cell-to-cell long-distance signaling in communities of unicellular algae and amoeba, as well as in ferns, mosses, mammalian cells, and isolated mouse hearts. The finding of a signaling process, like the ROS wave, in mammalian cells contributes to our understanding of different diseases and is likely to impact the development of drugs that target cancer or heart disease.

Author affiliations: [a]Division of Plant Sciences and Technology, College of Agriculture Food and Natural Resources and Interdisciplinary Plant Group, Christopher S. Bond Life Sciences Center, University of Missouri, Columbia, MO 65201; and [b]Department of Surgery, University of Missouri School of Medicine, Christopher S. Bond Life Sciences Center, University of Missouri, Columbia, MO 65201

[1]To whom correspondence may be addressed. Email: mittlerr@missouri.edu.

from one plant to another, provided that plants physically touch each other and conditions are humid (22). In addition to plasma membrane (PM)-localized RBOHs, the ROS wave requires the function of PD-localized proteins, calcium channels and signaling proteins, peroxiporins (aquaporins), phytochrome B, and the PM-localized apoplastic H_2O_2 receptor H_2O_2–induced Ca^{2+} increases 1 (HPCA1) protein (21, 23, 24). Numerous studies have shown that the ROS wave is linked to cell-to-cell calcium and electric signaling and that it is required for plant acclimation to stress (e.g., refs. 17, 21, 24–27).

As ROS such as $O_2^{.-}$, H_2O_2, $^1O_2$, and $HO^.$ are thought to have been present on Earth for billions of years and to have accompanied the evolution of unicellular and multicellular organisms (28–32), we hypothesized that ROS, and perhaps a ROS-driven rapid cell-to-cell signaling mechanism, like the ROS wave, could have evolved early during the evolution of life on Earth. To test this hypothesis, we studied whether ROS, and in particular a process like the ROS wave, could be found in plant lineages that diverged early in the plant phylogeny, including gymnosperms, ferns, bryophytes, multi and unicellular algae, as well as across the animal lineages in amoeba, mammalian cells, and isolated hearts from mice. Here, we show that a rapid ROS-mediated cell-to-cell signaling process can be found in all organisms included in this study, suggesting that ROS are evolutionarily conserved cell-to-cell stress signals.

Results

ROS as a Rapid Systemic Signal in Vascular and Nonvascular Plants. We previously identified and studied the ROS wave in several different angiosperm species including Arabidopsis, rice, tomato, maize, and dandelion (20, 22, 24, 33). However, whether ROS can function as a rapid systemic signal in gymnosperms, as well as other plant lineages, is unknown. Here, we show that a rapid systemic ROS signal can be triggered by a local treatment of high light (HL) stress in *Pinus sylvestris* (a Gymnosperm), *Azolla filiculoides* (a fern), and *Selaginella moellendorffii* (a Lycopodiaceae; *SI Appendix*, Fig. S1). The average rate of the ROS signal measured in these organisms is 0.14 cm min^{-1} (Table 1), faster than the diffusion rate of H_2O_2 in water or biological systems (the diffusion coefficient of H_2O_2 in water or tissues is in the range of 1 to 2.5 10^{-5} cm^2 min^{-1}; refs. 34–36), supporting the active nature of this systemic signal. The findings presented in Table 1 and *SI Appendix*, Fig. S1 suggest that rapid systemic ROS signaling is conserved across several different members of the vascular plant family and may have evolved before these lineages diverged from a common ancestor.

Although the ROS wave was shown to primarily propagate through the vascular bundles of Arabidopsis in response to a local HL stress (37), in response to a local wounding or heat stress (HS) treatments, it could also propagate through nonvascular tissues (i.e., mesophyll cells; ref. 38). We therefore extended our study to include Bryophytes (hornworts, liverworts, and mosses) that emerged from an early split in the diversification of land plants and lack lignified vascular tissues (39). A localized treatment of HL caused the activation of a rapid systemic ROS signal in *Anthoceros agrestis* (a Hornwort), *Marchantia polymorpha* (a Liverwort), and *Physcomitrium patens* (a Moss), with an average velocity of 0.13 cm min^{-1} (Fig. 1*A* and *SI Appendix*, Fig. S2 and Table 1). These findings suggest that rapid systemic ROS signals are conserved across all land plants and can spread in a systemic manner even in plants that lack a true vascular tissue.

Rapid Systemic ROS Signaling in Multicellular Algae and Unicellular Organisms. The findings that rapid systemic ROS signals are conserved among many land plants (Fig. 1 and

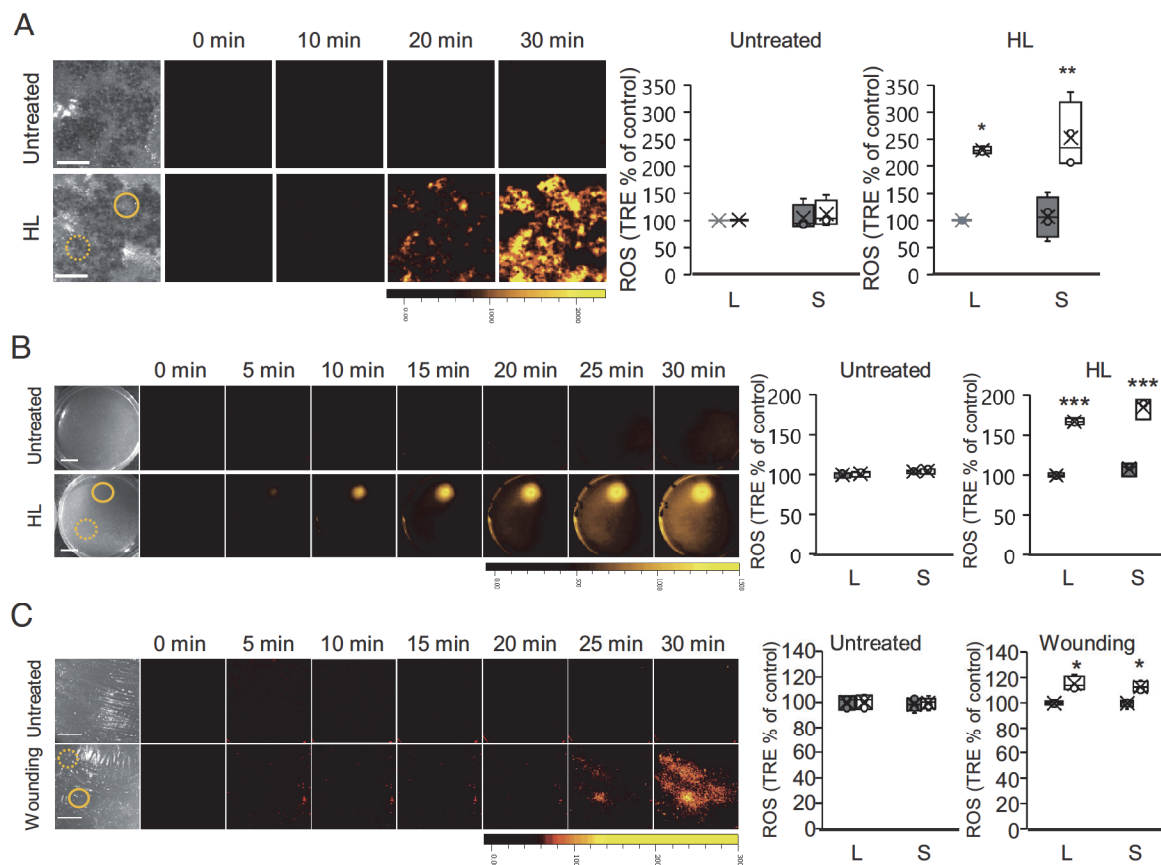**Table 1. Rates of the ROS wave in the different organisms studied**

Clade	Organism	Treatment	Average rate (cm min^{-1})
Amoebozoa	*D. discoideum*	Wounding/H_2O_2	0.2/0.09
Algae	*C. reinhardtii*	HL/H_2O_2	0.15/0.12
Algae	*C. vulgaris*	HL	0.14
Moss	*P. patens*	HL/H_2O_2	0.17/0.11
Hornwort	*A. agrestis*	HL	0.11
Liverwort	*M. polymorpha*	HL	0.12
Lycopodia	*S. moellendorffii*	HL	0.14
Ferns	*A. filiculoides*	HL	0.1
Gymnosperm	*P. sylvestris*	HL	0.18
Angiosperm	*A. thaliana*	HL	0.125
Eumuroida	*R. norvegicus* (H9c2)	Wounding	0.19
Eumuroida	*Mus musculus* (hearts)	Wounding	0.1
Primates	MDA-MB-231 (human)	Wounding	0.29

SI Appendix, Figs. S1 and S2, and Table 1; refs. 20, 22, 24, and 33) prompted us to test whether they can also be found in multicellular (*Chara vulgaris*) and unicellular (*Chlamydomonas reinhardtii*) algae. Multicellular and unicellular algae are known to use extracellular H_2O_2 as signals and contain NOX/RBOH enzymes (40, 41). A localized treatment of HL stress caused the activation of a rapid systemic ROS response in *C. vulgaris* grown in liquid medium (*SI Appendix*, Fig. S2*C*; velocity of 0.14 cm min^{-1}; Table 1), as well as in *C. reinhardtii* grown as a lawn on an agar plate (Fig. 1*B*; velocity of 0.12 cm min^{-1}; Table 1). These findings suggest that ROS can be used as a rapid systemic signal even by unicellular organisms and may have evolved as a cell-to-cell signaling mechanism before multicellularity emerged.

The findings that rapid systemic H_2O_2 signaling can be found in unicellular alga (Fig. 1*B*) prompted us to test whether it can also be found in other unicellular organisms, such as the soil-dwelling amoeba *Dictyostelium discoideum*, that contains NOX and uses extracellular H_2O_2 for signaling (41–43). A localized treatment of heat injury caused the activation of a rapid systemic ROS signal in the amoeba *D. discoideum* grown on agar plates (Fig. 1*C*; velocity of 0.2 cm min^{-1}; Table 1).

Initiation and Inhibition of the ROS Wave in *Physcomitrella*, *Chlamydomonas*, and *Dictyostelium*. Two important characteristics of the ROS wave are that it can be triggered by a localized application of H_2O_2, and that once activated, it can be blocked by the application of diphenyleneiodonium chloride (DPI; a broad-spectrum NOX/RBOH inhibitor) at a distant location away from its initiation site (19–21). Application of a 1 µL drop of 10 mM H_2O_2 to *Physcomitrella*, *Chlamydomonas*, or *Dictyostelium*, grown on agar plates, triggered a rapid systemic ROS signal (*SI Appendix*, Fig. S3). In contrast, application of mock buffer to cells, or application of 1 µL drop of 10 mM H_2O_2 to agar plates that contain no cells, did not result in a ROS signal (*SI Appendix*, Fig. S3). To test for H_2O_2 diffusion on plates that had no cells grown on them (live cells are required for H_2DCFDA imaging; ref. 44), we used 2′,7′-dichlorodihydrofluorescein (DCF; OxyBurst; 50 µM; refs. 19 and 20) to
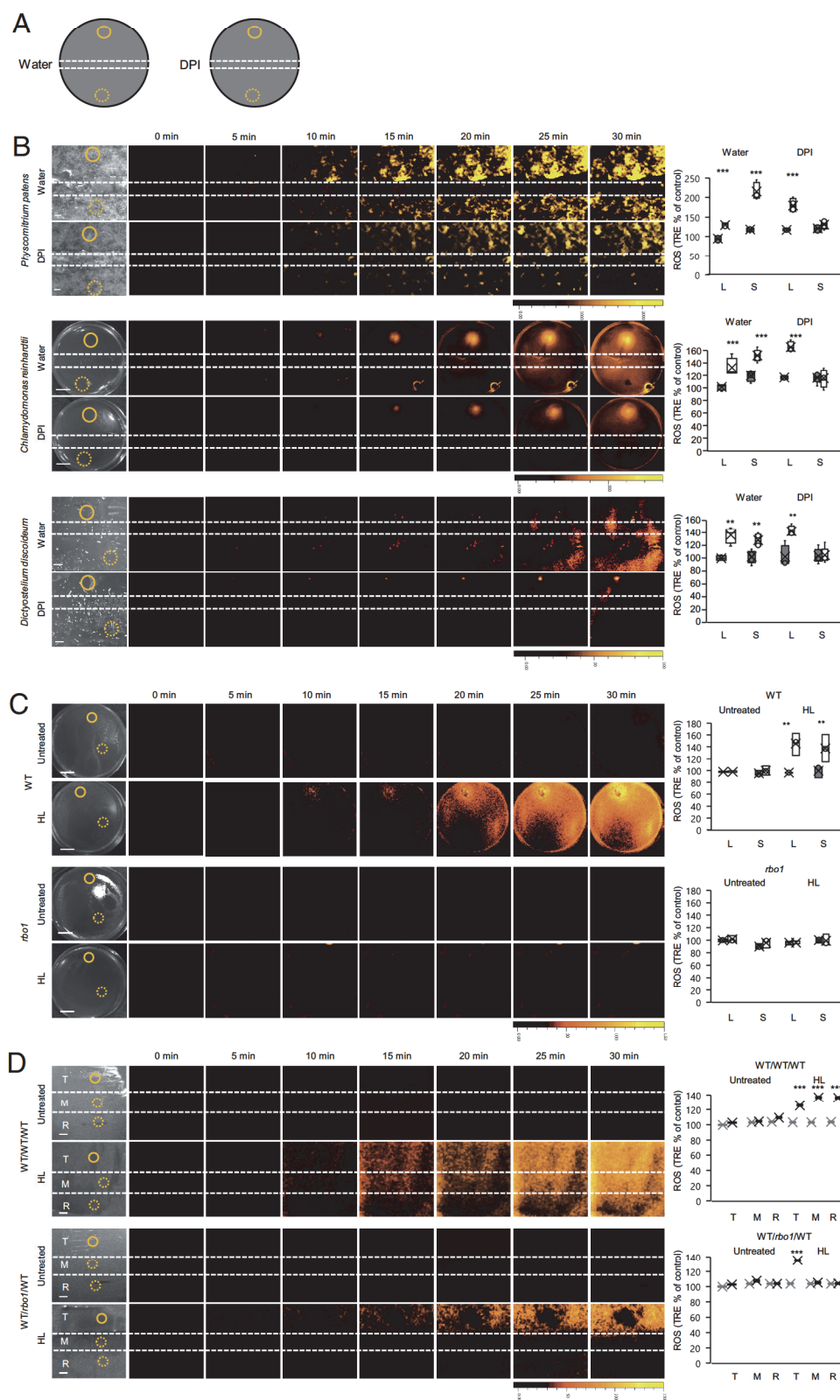
Fig. 1. Rapid systemic ROS signaling in *P. patens*, *C. reinhardtii*, and *D. discoideum*. (*A*) *P. patens*, a moss growing on an agar plate, was subjected to a HL stress treatment applied using a fiber optic to a single branch, and ROS accumulation was imaged, using H_2DCFDA, in the entire plate (local and systemic tissues are indicated with solid and dashed circles, respectively). Representative time-lapse images of whole moss ROS accumulation in treated and untreated areas are shown alongside bar graphs of combined data from all plates used for the analysis at the 0- and 30-min time points (local and systemic). (*B*) An agar plate containing a lawn of *C. reinhardtii*, a unicellular alga, was treated with a focused beam of HL (local treatment), and ROS accumulation was imaged using H_2DCFDA in the entire plate (local and systemic tissues are indicated with solid and dashed circles, respectively). Representative time-lapse images of whole plate ROS accumulation of treated and untreated *Chlamydomonas* lawn are shown alongside bar graphs of combined data from all plates used for the analysis at the 0- and 30-min time points (local and systemic). (*C*) Same as in (*B*), but for an agar plate that contains a lawn of *D. discoideum* that was treated locally with a heated rod (local). All experiments were repeated at least three times with 10 agar plates per experiment. Data are presented in (*A*–*C*) as box plot graphs; X is mean ± SE, N = 30, *$P < 0.05$, **$P < 0.01$, ***$P < 0.001$, Student *t* test. (Scale bar, 1 cm.) Abbreviations: H_2DCFDA, 2′,7′-dichlorodihydrofluorescein diacetate; HL, high light; L, local; ROS, reactive oxygen species; S, systemic; TRE, total radiant efficiency.

image ROS in empty plates following the application of 1 µL of 10 mM, or 1 M H_2O_2. We could not detect the 1 µL of 10 mM H_2O_2 (*SI Appendix*, Fig. S4), a concentration that resulted in a detectable ROS signal in plates with the different organisms (*SI Appendix*, Fig. S3), but were able to detect the 1 µL of 1 M H_2O_2 (*SI Appendix*, Fig. S4). This finding suggests that the living cells of the different organisms shown in *SI Appendix*, Fig. S3 amplified the 1 µL of 1 mM H_2O_2 to detectable levels via the ROS wave process.

To test the effect of DPI on the propagation of the rapid systemic ROS signal in *Physcomitrella*, *Chlamydomonas*, or *Dictyostelium*, grown on agar plates, we applied water or DPI (50 µM) in a 1-mm wide strip of agar to the middle of plates, waited 5 min and applied HL or heat injury at one end of the plate (Fig. 2*A*). Application of DPI (but not water) to the middle of the plates blocked the progression of the cell-to-cell ROS signal (after it was already initiated by the stress; Fig. 2*B*). To further test whether the ROS signal observed in *Chlamydomonas* in response to a local HL treatment (Figs. 1*B* and 2*B*) is mediated by an RBOH enzyme (as suggested by Fig. 2*B*), we subjected an *rbo1 C. reinhardtii* mutant (lmj.ry0402.234817) to a localized HL treatment. In contrast to wild type (WT), the RBOH/NOX *rbo1* mutant did not accumulate local or systemic ROS in response to the HL treatment (Fig. 2*C*). The *rbo1* mutant also failed to transfer an HL-induced cell-to-cell

ROS signal from one group of WT *Chlamydomonas* cells to another, further supporting the involvement of an RBOH enzyme in the propagation of cell-to-cell ROS signaling in *Chlamydomonas* (Fig. 2*D*). To test the effects of culture density on the ROS wave in *Chlamydomonas*, we grew *Chlamydomonas* lawns using different dilutions of cells and measured the rate of the ROS wave in them in response to a local HL stress treatment (*SI Appendix*, Fig. S5). This analysis revealed that even diluted lawns (10^{-3} dilution; *SI Appendix*, Fig. S5) activated the ROS wave in response to the local HL stress treatment (with an even higher intensity, potentially due to their higher levels of active metabolism required for cell division and growth). The findings presented in Fig. 2 and *SI Appendix*, Figs. S3 and S4 strongly suggest that the rapid systemic ROS signal, observed as propagating from the initial site of HL/heat injury in the different organisms, is autopropagating and resembles the ROS wave discovered in *Arabidopsis thaliana* (19–21, 37, 38).

Functional Analysis of the Rapid Cell-to-Cell Systemic ROS Signal in *Chlamydomonas*. To test whether the systemic ROS signal observed in *C. reinhardtii* (Fig. 1*B* and *SI Appendix*, Fig. S3) can transfer a biologically relevant signal between different cells that are at two ends of the signal path (i.e., local and systemic, on two
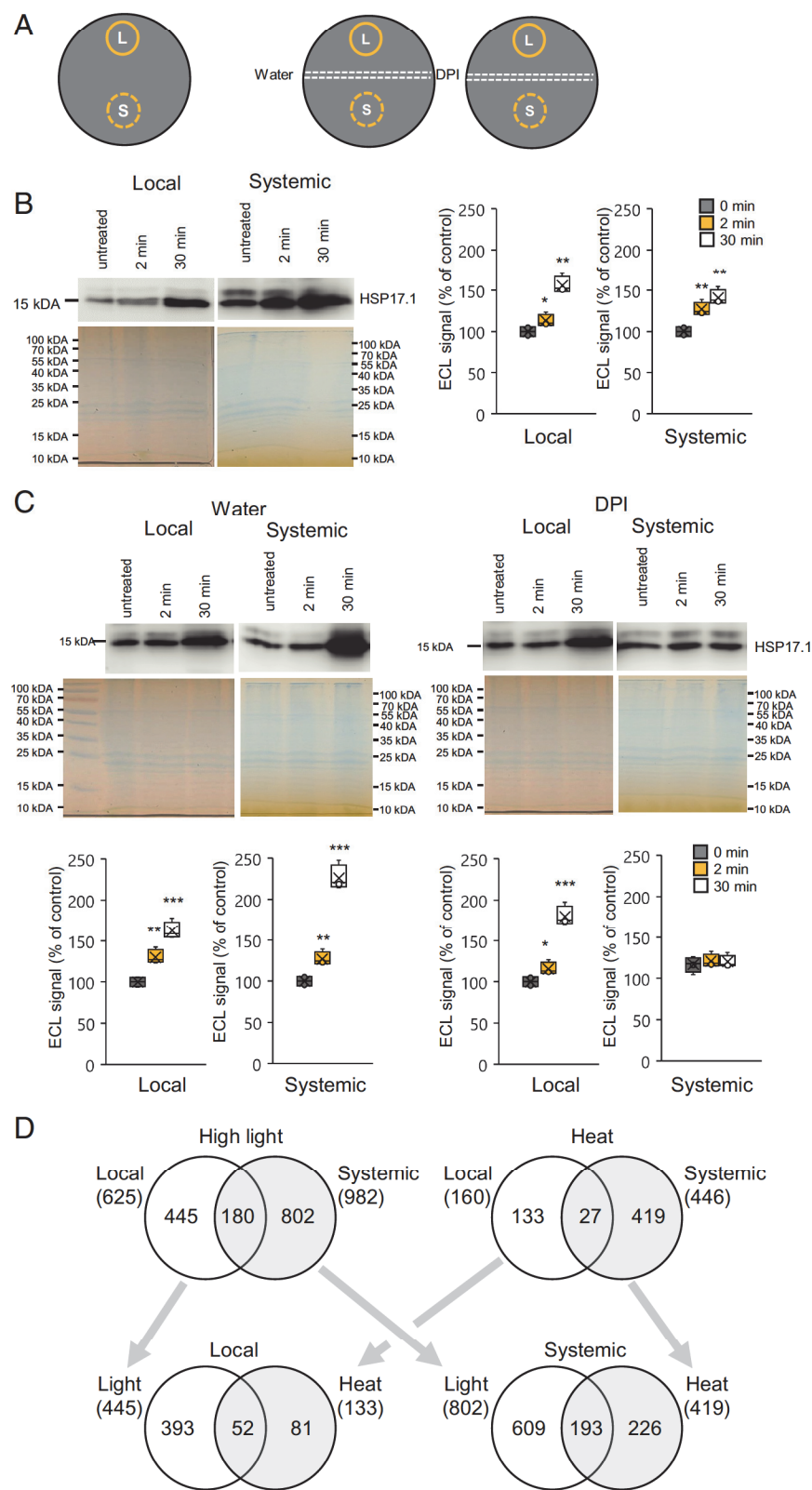
Fig. 2. Inhibition of the rapid systemic ROS signal in *P. patens*, *C. reinhardtii*, and *D. discoideum* by DPI, and suppression of the systemic rapid ROS signal in the *Chlamydomonas rbo1* mutant. (*A*) A diagram showing the experimental design used for (*B*). A strip of agar containing water or the NOX/RBOH inhibitor DPI (50 μM) was layered over the middle of agar plates containing a lawn of the different organisms. Following a 5-min incubation, one side of the plate was treated with a focused beam of HL or touched with a heated rod (local), and ROS accumulation was imaged using H$_2$DCFDA in the entire plate. Local and systemic locations used for signal quantification are indicated with solid and dashed circles, respectively. (*B*) Representative time-lapse images of whole plate ROS accumulation are shown alongside bar graphs of combined data from all plates used for the analysis at the 0- and 30-min time points (water or DPI-treated *P. patens*, *C. reinhardtii*, or *D. discoideum*; top, middle, and bottom, respectively; local and systemic). (*C*) Representative time-lapse images of whole plate ROS accumulation are shown alongside bar graphs of combined data from all plates used for the analysis at the 0- and 30-min time points of WT and the *rbo1* mutant of *Chlamydomonas* treated or untreated with a focused beam of HL stress. Local and systemic locations used for signal quantification are indicated with solid and dashed circles, respectively. (*D*) Same as in (*C*), but for plates that contained alternating populations of WT and the *rbo1* mutant in different combinations (WT, WT, WT, and WT, *rbo1*, WT). In all cases, the WT population on one side of each plate (*Top*) was treated or untreated with HL stress. Local (transmitter, T) and systemic (mediator, M; receiver, R) locations used for signal quantification are indicated with solid and dashed circles, respectively. All experiments were repeated at least three times with 10 agar plates per experiment. Data are presented in *B–D* as box plot graphs; X is mean ± SE, N = 30, **$P < 0.01$, ***$P < 0.001$, Student *t* test. (Scale bar, 1 cm.) Abbreviations: DPI, diphenyleneiodonium; H$_2$DCFDA, 2′,7′-dichlorodihydrofluorescein diacetate; HL, high light; L, local; M, mediator; NOX, NADPH oxidase; R, receiver; RBO, respiratory burst oxidase; ROS, reactive oxygen species; S, systemic; T, transmitter; TRE, total radiant efficiency; WT, wild type.

ends of the agar plate; Fig. 3*A*), we applied HL stress to one corner of a lawn of *Chlamydomonas* cells and sampled these cells, as well as cells that are on the other end of the plate (i.e., not subjected to the HL stress treatment; Fig. 3*A*). We then tested the expression of an HL-response small heat shock protein (sHSP17.1) in cells located at the two ends of the signal path following the application of HL stress to one end of the plate (stressed cells; local). The expression of sHSP17.1 was elevated at both ends of the signal path (local and

systemic; Fig. 3*A*) suggesting that the ROS wave signal connecting these cells is conveying a stress response signal from the stressed (local) to the nonstressed (systemic) cells (Fig. 3*B*).

To test whether inhibiting the ROS wave in *Chlamydomonas* growing on an agar plate (Figs. 1*B* and 2 *B* and *C* and *SI Appendix*, Fig. S3) would inhibit the transfer of the stress–response signal from one side of the plate to the other (Fig. 3*B*), we applied DPI (50 μM) or water at the middle point between the stressed cells

Fig. 3. Functional analysis of the cell-to-cell rapid ROS signal in *C. reinhardtii*. (*A*) Diagrams showing the experimental designs used. *Left*: A lawn of *C. reinhardtii* growing on an agar plate was subjected to a focused beam of HL stress and the area subjected to the beam (local, L), as well as an area that is on the other end of the plate (systemic, S) were sampled at different times following the application of HL for analysis of the expression of the light stress response small heat shock protein 17.1 (sHSP17.1; This design was used for the experiments shown in *B*). *Right*: A strip of agar containing water or the NOX/RBOH inhibitor DPI (50 μM) was layered over the middle of agar plates containing the lawn of *C. reinhardtii* 5 min prior to the application of light stress and sampling (This design was used for the experiments shown in *C*). Local and systemic sampling locations are indicated with solid and dashed circles, respectively. (*B*) Representative protein blots and Coomassie-stained gels are shown alongside bar graphs of combined data from all blots used for the analysis at the 0-, 2-, and 30-min time points, for the expression of sHSP17.1 in the L and S locations, following the light stress treatment. (*C*) Same as in *B*, but for experiments in which a strip of agar containing water (*Left*) or DPI (*Right*) was layered over the middle of agar plates 5 min prior to the application of HL stress. (*D*) Venn diagrams showing changes in protein abundance in local and systemic cells (following the experimental design shown in *A*, left panel), treated or untreated at the local area with HL or HS for 10 min and sampled at 30 min following the end of the local stress treatment. See text for more details. All experiments were repeated at least three times with 10 agar plates per experiment. Data are presented in (*B* and *C*) as box plot graphs; X is mean ± SE, N = 30, *P < 0.05, **P < 0.01, ***P < 0.001, Student t test. (Scale bar, 1 cm.) Abbreviations: DPI, diphenyleneiodonium; H₂DCFDA, 2′,7′-dichlorodihydrofluorescein diacetate; HL, high light; HS, heat stress; L, local; NOX, NADPH oxidase; RBOH, respiratory burst oxidase homolog; ROS, reactive oxygen species; S, systemic; sHSP, small heat shock protein.

and the cells that did not sense the stress (like Fig. 2). DPI, but not water, inhibited the expression of sHSP17.1 in the systemic cells following the application of HL stress to the local cells (Fig. 3*C*). In contrast, DPI or water did not inhibit the expression of sHSP17.1 at the stressed local cells (Fig. 3*C*). These findings suggest that the cell-to-cell ROS signal connecting the two ends of the *Chlamydomonas* lawn transfers biologically relevant signals between cells.

To determine the depth of information potentially transferred between the local and systemic *Chlamydomonas* cells growing on an agar plate (Fig. 3 *A*–*C*), we conducted proteomics analysis of these cells 0 and 30 min following the application of a 10 min HL or HS to local cells (Fig. 3*D* and Datasets S1–S12). The HL treatment resulted in a significant change in the abundance (accumulated or decreased) of 625 and 982 proteins in local and systemic cells, respectively, with an overlap of 180 proteins (28.8%;

Fig. 3D and Datasets S1–S3). In contrast, the HS treatment resulted in a significant change in the abundance (accumulated or decreased) of 160 and 446 proteins in local and systemic cells, respectively, with an overlap of 27 proteins (16.8%; Fig. 3D and Datasets S4–S6). The findings presented in Fig. 3D reveal that many proteins that respond to the stress at the local cells also respond to it in the systemic cells. Interestingly, 193 proteins were common to the systemic response of *Chlamydomonas* cells to HL or HS (Fig. 3D and Dataset S12). As HS also triggered a ROS wave in a lawn of *Chlamydomonas* cells (*SI Appendix*, Fig. S6), these proteins could be under its control. Among the 193 proteins common to the systemic responses of *Chlamydomonas* cells to HL and HS were the ROS-related proteins thioredoxin, peroxiredoxin, superoxide dismutase, sHSP, and ferredoxin (Dataset S12).

Cell-to-Cell ROS Signaling in Mammalian Cells and Isolated Hearts. The finding of the ROS wave in *Dictyostelium* (Figs. 1C and 2B and *SI Appendix*, Fig. S3C) demonstrated that organisms that are outside the plant and algal lineages could use ROS as a cell-to-cell signal. *Dictyostelium* was previously found to contain an ancestral form of NOX (28, 41, 43), suggesting that other organisms that contain NOX enzymes (e.g., mammalian cells) could use ROS for rapid cell-to-cell signaling. To test this possibility, we studied cell-to-cell ROS signaling in monolayers of human (*Homo sapiens*) epithelial breast cancer cells (MDA-MB-231) and rat (*Rattus norvegicus*) cardiomyocytes (H9c2) grown in culture. Wounding of a monolayer of MDA-MB-231 or H9c2 cells with a heated rod resulted in a ROS signal that spread from the injury site at a velocity of 0.28 or 0.2 cm min^{-1}, respectively (Fig. 4A and Table 1). In the case of H9c2 cells, the ROS signal appeared to travel away from the wound site and to do so in a directional manner, suggesting that it is not simply H_2O_2 that is diffusing away from the initial wound site in all directions (Fig. 4A and Movie S1). To test whether the spreading ROS signal is a result of cell migration and/or monolayer detachment, we conducted microscopic analyses of H9c2 cells at the end the ROS imaging experiments. This analysis revealed that the wound site had an average diameter of 300 to 600 μm and that cells did not detach or migrate away from it (*SI Appendix*, Fig. S7). Moreover, migration of cells away from the wound site would have been much slower (1–10 μm min^{-1}; ref. 45) than the rate of the signal observed (0.2 cm min^{-1}; Table 1). In addition, to test whether ROS can be detected in all H9c2 cells growing on the plates (not only the cells observed generating ROS after wounding; Fig. 4A and Movie S1), we treated the entire plate with a final concentration of 1 mM H_2O_2 at the end of the experiment (*SI Appendix*, Fig. S8). This analysis revealed that all cells on the plate were able to uptake the H_2DCFDA dye and that H_2O_2 that was provided to the media and entered cells generated a signal (for H_2DCFDA to generate a signal it has to enter live cells; ref. 44). To test whether the ROS signal observed in MDA-MB-231 or H9c2 is associated with NOX function, we applied DPI (50 μM) or buffer (mock) to these cells prior to the heat injury. DPI, but not buffer, caused the complete suppression of the ROS signal (Fig. 4B). As DPI is a broad-range NOX inhibitor (46, 47), we also applied the two specific mammalian NOX inhibitors, APX115 (50 μM) and/or Setanaxib (50 μM), to MDA-MB-231 or H9c2 cells grown as a monolayer prior to the heat injury. Application of APX115 or Setanaxib did not completely suppress the ROS wave in these cells (*SI Appendix*, Fig. S9), while application of APX115+Setanaxib did (Fig. 4B and *SI Appendix*, Fig. S9). These findings suggest that NOX1 or NOX2, and NOX4 might be involved in mediating the ROS wave in mammalian cells.

The finding of a ROS wave-like signaling process in rat cardiomyocytes grown in culture (Fig. 4 A and B and Movie S1) prompted us to test whether a similar process could be found in isolated mice hearts. For this purpose, we collected hearts from 9- to 10-wk-old female and male C57BL/6 J mice and incubated them with H_2DCFDA for 2 h. We then wounded the isolated hearts using an open-flame-heated rod and imaged ROS responses in the entire heart. Wounding of isolated mice hearts resulted in a rapid ROS response that originated from the point of wounding and progressed at an average rate of 0.106 cm min^{-1} to other parts of the heart (Fig. 4C and *SI Appendix*, Fig. S10 and Table 1 and Movie S2). This process was inhibited by DPI application to hearts 30 min prior to wounding (Fig. 4C and *SI Appendix*, Fig. S10). These findings suggest that a ROS wave-like signaling process could occur in isolated heart tissue.
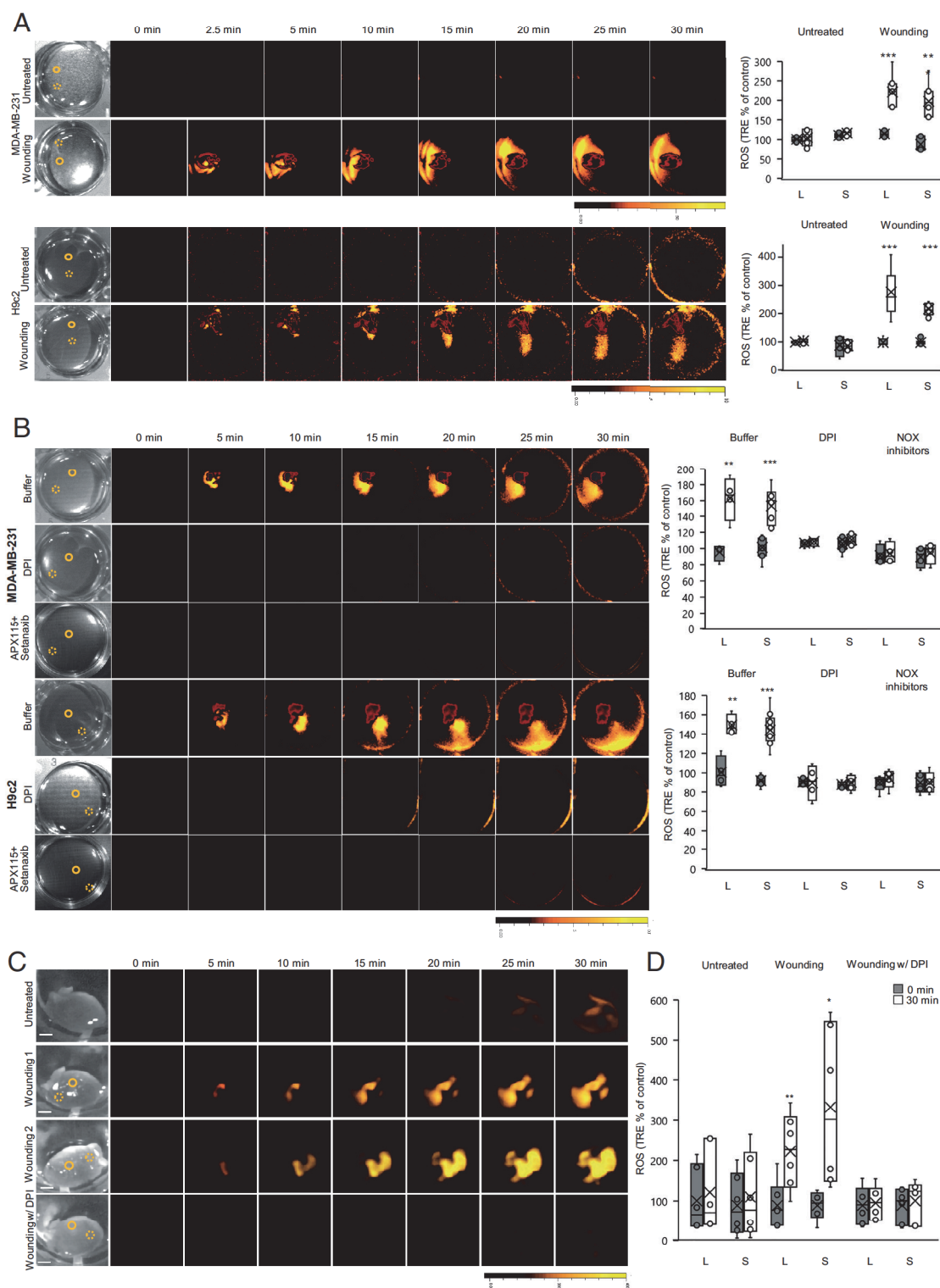
Identification of H_2O_2 as the ROS Mediating Rapid Cell-to-Cell Signaling in Mammalian Cells, Isolated Hearts, and *Chlamydomonas*. As H_2DCFDA is a broad-spectrum dye used for H_2O_2/ROS detection (44, 46, 47), we studied the ROS wave in H9c2 cells grown as a monolayer, *Chlamydomonas* grown as a lawn, and isolated mice hearts, using the H_2O_2-specific boronate–based caged fluorescent probe Peroxy Orange 1 (PO1; 20 μM; Fig. 5 and Movie S3; refs. 46 and 47). In addition, to determine whether H_2O_2 is the ROS being mobilized between cells extracellularly, we conducted our H_2O_2 imaging analysis with PO1 in the presence or absence of the H_2O_2-specific scavenger catalase (100 U/mL). A similar pattern of systemic cell-to-cell H_2O_2 signaling was observed in the different experimental systems imaged with PO1 or H_2DCFDA (Figs. 4 and 5 and *SI Appendix*, Fig. S9 and Movies S1–S3). In addition, catalase blocked the spread of the ROS wave in all systems studied in Fig. 5. These findings identified H_2O_2 as the ROS being mobilized between cells during rapid cell-to-cell signaling.
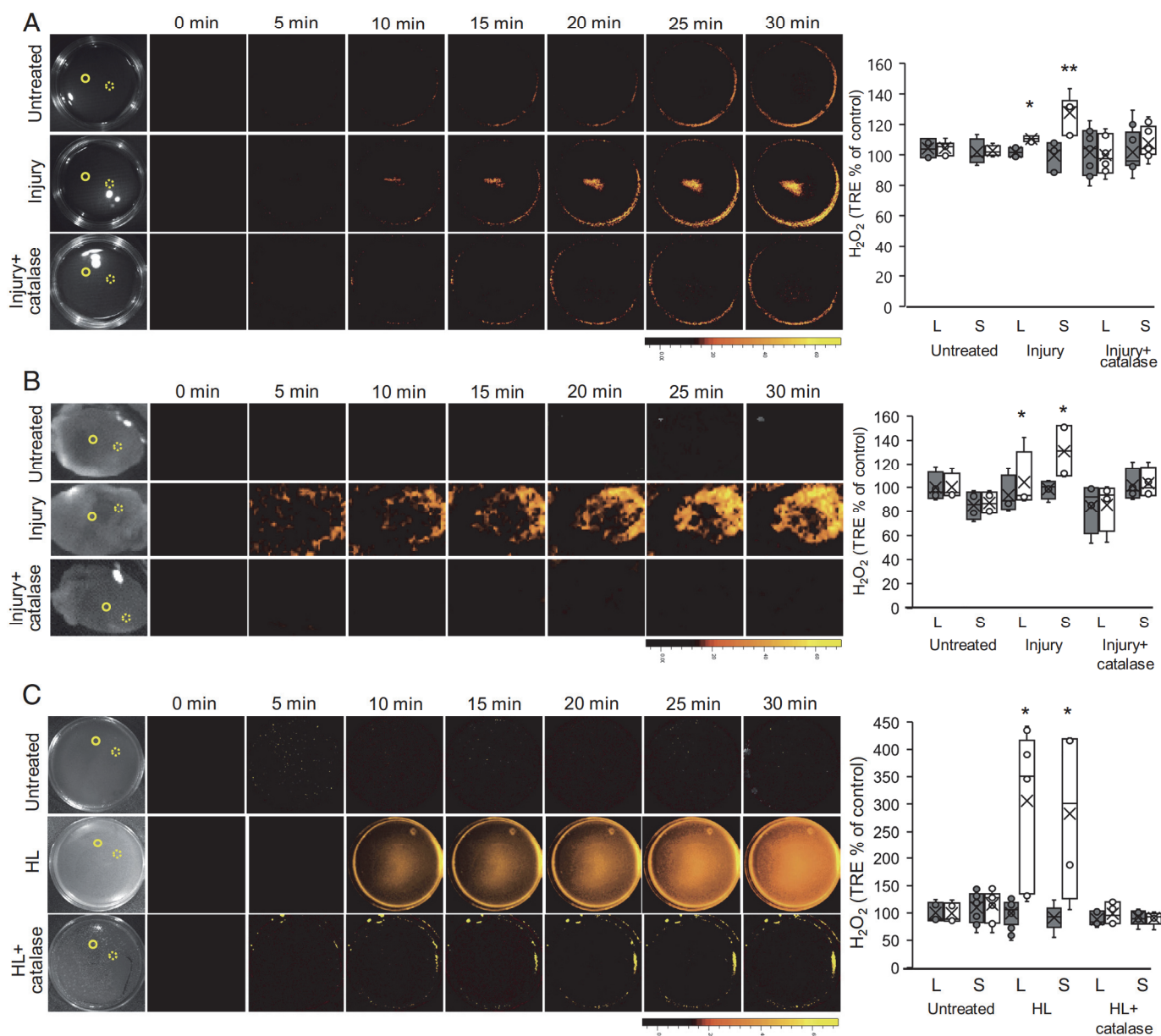
Discussion

The steady-state level of H_2O_2 in cells can vary in response to different environmental conditions, the activation of developmental programs that cause active production of H_2O_2, and/or a decline in the activity of H_2O_2 scavenging mechanisms (46–50). H_2O_2 can also diffuse into or out of cells through peroxiporins, and most aquaporin channels, further impacting intracellular H_2O_2 levels (46–50). Because H_2O_2 affects the redox state of cells and can alter gene expression through oxidative posttranslational modifications (oxi-PTMs) of different proteins (46–50), it functions as a key signal transduction molecule involved in the sensing of stress and/or the activation of different developmental programs (46–50).

As H_2O_2 can be transported in or out of cells through peroxiporins and/or other channels/pores, secretion or extracellular production of H_2O_2 by one cell can alter the redox state of a neighboring cell, thereby altering gene expression within it. This type of paracrine signaling is thought to play an important role in cell-to-cell signaling occurring in different communities of microorganisms, during algal blooms, during interactions between neurons, or during the recruitment of leukocytes to wound sites (51–56). A central feature of this paracrine signaling mechanism is however that it depends on a gradient of H_2O_2 forming from the secreting/producing cell(s) to the receiving cell(s) (56). In addition, H_2O_2 can be scavenged in route from one cell to the other, limiting the range of this signaling pathway. Having the ability to amplify and maintain cell-to-cell H_2O_2 signals, like the autopropagating ROS wave process in plants (19–21, 37, 38), could improve

Fig. 4. Rapid systemic ROS signaling in mammalian cells and isolated mouse hearts. (*A*) Monolayers of human epithelial breast cancer (MDA-MB-231; *Top*), and rat cardiomyocytes (H9c2; *Bottom*); cells grown in culture were treated with a heated metal rod to induce injury (average injury diameter is 120 μm), and ROS accumulation was imaged using H$_2$DCFDA in the entire plate. Representative time-lapse images of whole plate ROS accumulation in treated and untreated plates are shown alongside bar graphs of combined data from all plates used for the analysis at the 0- and 30-min time points (local and systemic). Local and systemic sampling locations are indicated with solid and dashed circles, respectively. (*B*) Same as in *A*, except that buffer, DPI (50 μM), or APX115 (50 μM) and Setanaxib (50 μM), were added to the growth media of cells 10 min prior to the heat injury. Results for APX115 or Setanaxib application are shown in *SI Appendix*, Fig. S8. All experiments were repeated at least three times with 10 agar plates per experiment. Data are presented in (*A* and *B*) as box plot graphs; X is mean ± SE, N = 30, **$P < 0.01$, ***$P < 0.001$, Student *t* test. (Scale bar, 1 cm.) (*C*, *D*) Mouse hearts, surgically removed from 9- to 10-wk-old male and female C57BL/6 J mice, were untreated, or treated with a heated metal rod (to induce injury), in the presence or absence of DPI (50 μM), and ROS accumulation was imaged using H$_2$DCFDA in the entire hearts. Representative time-lapse images of whole heart ROS accumulation are shown alongside bar graphs of combined data from all hearts used for the analysis at the 0- and 30-min time points. Local and systemic sampling locations are indicated with solid and dashed circles, respectively. All experiments were repeated at least three times with three female and three male mice per experiment. Data are presented as box plot graphs; X is mean ± SE, N = 30, **$P < 0.01$, ***$P < 0.001$, Student *t* test. (Scale bar, 1 cm.) Female- and male-specific ROS responses are shown in *SI Appendix*, Fig. S9. Abbreviations: DPI, diphenyleneiodonium; H$_2$DCFDA, 2′,7′-dichlorodihydrofluorescein diacetate; L, local; ROS, reactive oxygen species; S, systemic; TRE, total radiant efficiency.
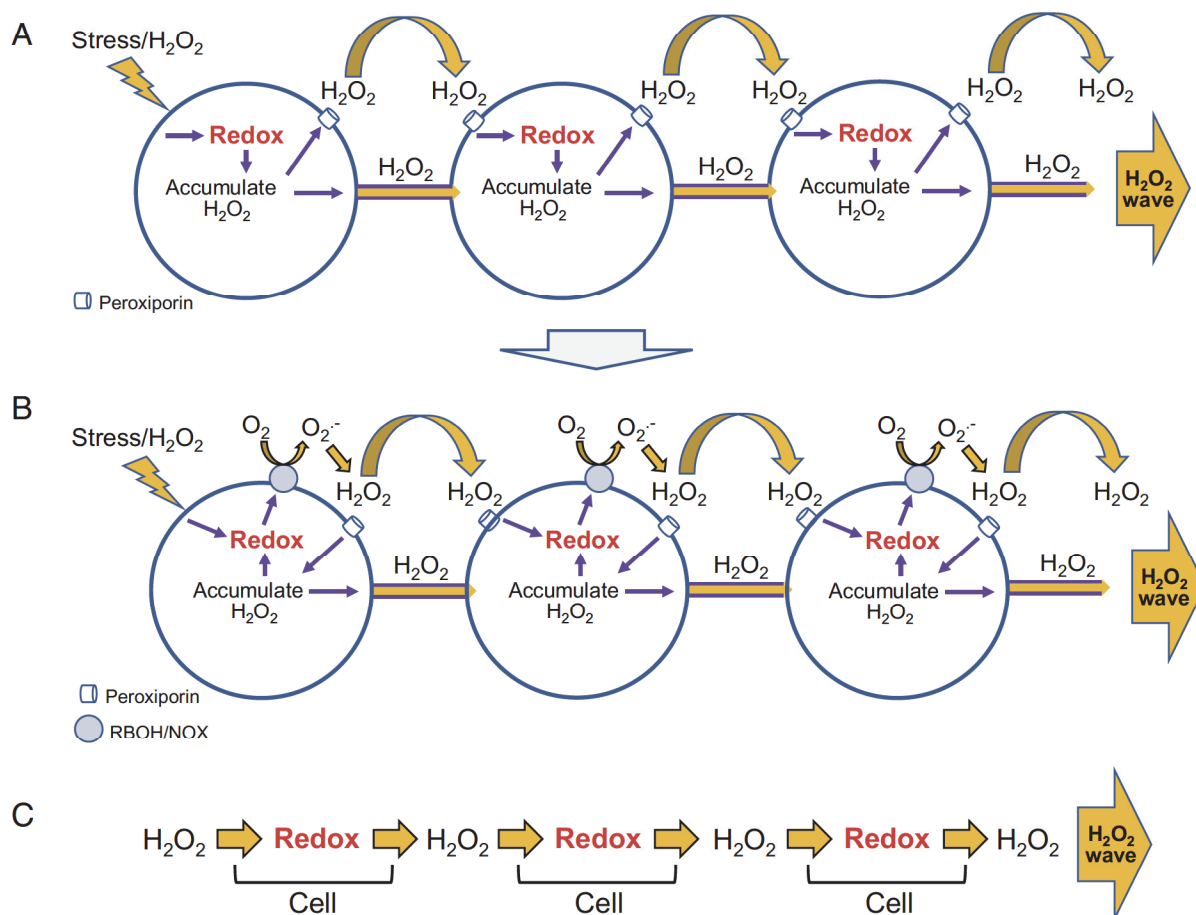
Fig. 5. Identification of H$_2$O$_2$ as the ROS mediating rapid cell-to-cell signaling in mammalian cells, isolated hearts, and *C. reinhardtii*. (*A*) Monolayers of rat cardiomyocytes (H9c2) cells grown in culture were treated or untreated with a heated metal rod to induce injury (as described in Fig. 4*A*), in the presence or absence of catalase (100 U/mL), and H$_2$O$_2$ accumulation was imaged using PO1 (20 µM) in the entire plate. Representative time-lapse images of whole plate H$_2$O$_2$ accumulation in treated and untreated plates are shown alongside bar graphs of combined data from all plates used for the analysis at the 0- and 30-min time points (local and systemic). Local and systemic sampling locations are indicated with solid and dashed circles, respectively. (*B*) Same as in *A*, but for isolated mouse hearts (treated or untreated as described in Fig. 4*C*). (*C*) Same as in *A*, but for *C. reinhardtii* cells grown as a lawn on agar plates and treated or untreated with HL stress (as described in Fig. 1*B*). All experiments were repeated at least three times with 10 agar plates per experiment. Data are presented in *A–C* as box plot graphs; X is mean ± SE, N = 15, **P < 0.01, ***P < 0.001, Student *t* test. (Scale bar, 1 cm.) Abbreviations: DPI, diphenyleneiodonium; H$_2$DCFDA, 2′,7′-dichlor odihydrofluorescein diacetate; HL, high light; L, local; PO1, Peroxy Orange 1; S, systemic; TRE, total radiant efficiency.

the communication between cells in a biofilm/community/tissue and allow them to respond faster and in unison (Fig. 6). Here, we demonstrate that *Physcomitrella*, *Chlamydomonas*, and *Dictyostelium*, growing on agar plates, and mammalian cells growing in culture, indeed have the capacity to amplify and maintain cell-to-cell H$_2$O$_2$ signals (Figs. 1–5 and *SI Appendix*, Figs. S3 and S9 and Table 1). We further show that cell-to-cell H$_2$O$_2$ signaling may also occur in monolayers of mammalian cells and in isolated mouse hearts (Figs. 4 and 5 and *SI Appendix*, Fig. S10). These findings suggest that the ROS wave signaling process, that was originally discovered in flowering plants (19–21, 37, 38), could have originated early in evolution and is conserved between plants, eukaryotic microorganisms, and animals. In support of this finding is the observation

that the systemic ROS signal could be initiated by H$_2$O$_2$ (*SI Appendix*, Fig. S3), that application of DPI at a location that is away from the initiation site could block it (Figs. 2–4 and *SI Appendix*, Figs. S9 and S10), and that it was suppressed in the *rbo1* mutant of *Chlamydomonas* (Fig. 2 *C* and *D*). Moreover, in H9c2 cells, the peak of the ROS signal propagated in a directional manner at a rate of 0.2 cm min^{-1} departing from its original initiation site and continuing to move away from it in a manner that clearly suggests it is not mediated by simple diffusion (Figs. 4 *A* and *B* and 5*A* and *SI Appendix*, Fig. S9 and Movies S1 and S3). Although the directionality of the ROS signal (Figs. 4 *A* and *B* and 5*A* and *SI Appendix*, Fig. S9 and Movies S1 and S3) could be related to cell polarity, it is unknown at present what is the

Fig. 6. A model depicting the principle of the cell-to-cell H_2O_2 signaling pathway that is conserved between unicellular and multicellular eukaryotic organisms. (*A*) Hypothetical origin of the cell-to-cell ROS signal in bacterial communities. (*B*) A proposed model for the cell-to-cell ROS signal in unicellular eukaryotes and multicellular organisms, following the evolution of NOX/RBOH enzymes. (*C*) The basic principle of ROS causing a redox change that cause more ROS production ("H_2O_2-redox-H_2O_2") common to the two models shown above. Please see text for more details. Abbreviations: oxi-PTM, oxidative posttranslational modification; NOX, NADPH oxidase; RBOH, respiratory burst oxidase homolog; ROS, reactive oxygen species.

mechanism that governs it. A similar directional spread of the ROS signal was also observed in isolated hearts (Figs. 4*C* and 5*B* and Movie S2), further supporting the notion that it is not a simple diffusion process. In addition, the rate of the ROS signal observed in hearts was also faster than that of H_2O_2 diffusion in biological systems or water (Table 1; refs. 34–36). Taken together, these findings suggest that the ROS signal observed in a monolayer of H9c2 cells (Figs. 4*A* and 5*A*), or isolated hearts (Figs. 4*C* and 5*B*), is driven by an active process of ROS production (that could be inhibited by NOX inhibitors or catalase; Figs. 4 and 5 and *SI Appendix*, Fig. S9), involving multiple cells along its path (i.e., not only cells at and around the injury site), and that this process could be linked with other cell-to-cell signals (e.g., calcium, electric signals, hormones, and/or different metabolites) that affect its directionality.

An interesting analogy to the cell-to-cell ROS wave signaling process of plants is the synchronized process of ROS flushes that occurs in mitochondria that are arranged in a lattice formation in muscle tissue (e.g., refs. 57 and 58). In this process, the release of H_2O_2 through pores of one mitochondrion results in the release of H_2O_2 from a neighboring mitochondrion spreading from mitochondria-to-mitochondria in a ROS-induced-ROS-release fashion (57, 58). In the context of our findings, that a similar process of cell-to-cell ROS signaling occurs in many different

unicellular and multicellular organisms, it is possible that even ancient prokaryotic organisms that were the progenitors of mitochondria used this type of cell-to-cell signaling to orchestrate responses within a biofilm or a colony (Fig. 6*A*). It is also possible that mitochondria are actively involved in the cell-to-cell ROS signal found in H9c2 cells or hearts and that NOXs such as NOX4 that is associated with mitochondria in mammalian cells (59) are mediating this process (Figs. 4 and 5 and *SI Appendix*, Fig. S9). Further studies are needed to address the potential role of mitochondria in cell-to-cell ROS signaling.

In addition to paracrine signaling, cells can use juxtacrine signaling to exchange H_2O_2 with each other (60). To use this route, however, the levels of H_2O_2 transported cannot be too high, as the transmitting or receiving cells could be damaged. Cells living within a biofilm, colony, and/or within different plant and animal tissues, are thought to use juxtacrine signaling to mediate cell-to-cell H_2O_2 and redox signaling (10, 11). Moreover, it was suggested that H_2O_2 can enhance the size of tunneling nanotubes or PDs and facilitate juxtacrine signaling (23, 60). Because we did not distinguish between paracrine and juxtacrine signaling in our study (aside from blocking the signal with catalase; Fig. 5), we cannot rule out the possibility that the different cells we imaged used one or the other, or both, for the process of cell-to-cell ROS signaling. In this respect it should be mentioned that our studies

of the ROS wave in plants revealed that for cell-to-cell paracrine ROS signaling to occur, juxtacrine signaling must also occur, as key proteins localized to the PD must be present (23). Paracrine and juxtacrine signaling might therefore be linked in other organisms and this aspect of cell-to-cell ROS signaling should be addressed in future studies.

Cancer cells use ROS to regulate their own proliferation and to communicate with cancer-associated macrophages and other host cells (e.g., ref. 61). In addition, ROS play a key role in cancer metastasis (e.g., ref. 62). Our findings that cancer cells can generate and transmit long-distance ROS signals (Figs. 4 and 5 and *SI Appendix*, Fig. S9), could suggest that a similar process may occur within the tumor microenvironment. This finding should be further studied as it may affect the development of cancer fighting drugs. In the heart, ROS are implicated in ischemia reperfusion (IR) injury, both in the acute setting of myocardial infarction (MI), as well as in the chronic remodeling process following a MI (e.g., refs. 63–65). Our findings that cardiomyocytes can use ROS for cell-to-cell communication (Figs. 4 and 5 and *SI Appendix*, Fig. S9 and Movies S1 and S3), and that an active process of ROS signaling is triggered in isolated hearts upon localized wounding (Figs. 4 and 5 and Movie S2), could suggest that enhanced ROS production during IR could trigger different ROS signals that would augment or suppress the tissue damage caused during IR injury. This finding should also be further studied as it could lead to the development of therapies that will limit tissue damage during or following IR.

Taken together, our findings suggest that cell-to-cell ROS signaling evolved before unicellular and multicellular organisms diverged (Figs. 1–5 and *SI Appendix*, Figs. S1–S3 and Table 1; refs. 19–24). Because ROS, such as H_2O_2, are thought to have been present on Earth for billions of years and are used to sense the cell's environment through changes in the redox status of the cell (28, 32, 46–50), it is possible that a cell-to-cell communication process that uses H_2O_2 as a signal emerged early in evolution (Fig. 6A). This mechanism could have conveyed an environmental stress signal that altered the redox state of one cell (the initiating cell) through H_2O_2 produced and secreted by this cell to an acceptor cell (Fig. 6A). The changes in redox state caused by the perceived H_2O_2 signal in the acceptor cell would therefore "mirror" the change in the redox state of the initiating cell, and information in the form of a "redox change" transmitted from one cell to the other (Fig. 6A). The changes in redox state occurring in each of the cells involved in this pathway could cause H_2O_2 accumulation and activate gene expression through oxi-PTMs linking the gene expression and H_2O_2 responses of both cells (Fig. 6A). As the redox state of other neighboring cells would also be altered in a similar manner during this process (like the redox changes that occur in cells along the path of the ROS wave in plants; ref. 66), and these cells will also start accumulating and secreting H_2O_2, the entire colony or biofilm would respond in unison to the stress perceived by the initiating cell (Fig. 6A), improving its chances of acclimation to the sensed stress, as well as overall survival. Such a mechanism could have coordinated the redox and H_2O_2 accumulation responses of a network of cells and given this cell population a better chance of survival in the early environment that was present on Earth. Once NOX-like enzymes evolved (28–32, 41, 43), an active process of extracellular ROS production could have overtaken the secretion of H_2O_2 from cells and made this process much more efficient and rapid (Fig. 6B). Regardless of whether it is ROS secretion (Fig. 6A) or ROS production (Fig. 6B), the principle of "H_2O_2-redox-H_2O_2" coordination is the underlying basis for the transmission of information by this cell-to-cell ROS communication pathway (Fig. 6C). The use of H_2O_2 as a signal to alter gene expression in response to

stress, depicted in Fig. 6, raises the possibility that H_2O_2 served as one of the first "stress hormones" on Earth (Fig. 6). Our findings that catalase or different inhibitors of NOXs can inhibit this process (Figs. 2–5 and *SI Appendix*, Figs. S9 and S10) support its active nature (19–21). We further show that systemic signaling can occur in a community of *Chlamydomonas* cells in response to HL or HS and that there is a considerable overlap between the stress-induced locally altered proteins and the proteins altered in systemic cells that did not directly sense the stress (about 30 and 17% overlap, in response to HL or HS, respectively; Fig. 3D). Moreover, the systemic responses of *Chlamydomonas* cells to HL or HS share about 190 proteins that could be regulated by the ROS wave, and this group of proteins contains ROS-related proteins such as superoxide dismutase, thioredoxin, and peroxiredoxin (Fig. 3D and Dataset S12). Compared to higher plants (25), *Chlamydomonas* cells appear, however, to have a much higher degree of overlap between systemic responses to HL or HS, suggesting that flowering plants can display a higher level of complexity in systemic signaling that allows for a higher degree of systemic stress specificity (Fig. 3D; ref. 25). Our study could also be viewed within the context of the overall "redox code" of cells (67), expanding its third principle, "Activation/deactivation cycles of H_2O_2 production," to include multiple cells communicating with each other within a tissue, and linking it to the fourth principle, "Adaptation to the environment," as these coordinated redox changes are in response to an external stress stimulus (Fig. 6).

Materials and Methods

Organisms and Stress Treatments. The following organisms were studied in this research: *P. sylvestris* (TreeHelp), *A. filiculoides* (Carolina Biological Supply Company), *S. moellendorffii* (Putnam Hill nursery), *M. polymorpha* (Carolina Biological Supply Company), *A. agrestis* (a kind gift from Prof. Fay-Wei Li, Cornell University, Ithaca, NY, USA), *P. patens* (a kind gift from Prof. Elisabeth Haswell, Washington University at St. Louis, St. Louis, MO, USA, and International Moss Stock Center, and Prof. Ralf Reski, University of Freiburg, Freiburg, Germany), *C. vulgaris* (Carolina Biological Supply Company), WT *C. reinhardtii* and the *rbo1 C. reinhardtii* mutant (lmj.ry0402.234817 from the Chlamydomonas Resource Center, University of Minnesota, St. Paul, MN, USA, and UTEX Culture Collection of Algae), *D. discoideum* (a kind gift from Prof. Thierry Soldati, University of Geneva, Geneva, Switzerland, and Carolina Biological Supply Company), and H9c2 and MDA-MB-231 (American Type Culture Collection (ATCC)). Organisms were grown according to stock resource instructions. Photosynthetic organisms were grown under 8 h/16 h light/dark regime. *P. sylvestris*, *S. moellendorffii*, and *M. polymorpha* were grown in peat pellets (Jiffy-7, Jiffy International, Kristiansand, Norway; refs. 20 and 21). *A. filiculoides* was grown in 0.25 Murashige & Skoog (MS) liquid media (68); *A. agrestis* was grown on a solid modified Hatcher medium (69); *P. patens* was grown on routine basal culture medium for moss (BCD) solid media (70); *C. vulgaris* was grown in a Broyer and Barr liquid media (71); *C. reinhardtii* cultures were grown on P49 solid media (UTEX Culture Collection of Algae); *D. discoideum* cultures were grown on Sussman's standard media (SM) agar plates in room temperature (72). Mammalian cells were grown in 37 °C 5% CO_2 Roswell Park Memorial Institute (RPMI) medium 1640 supplemented with 10% FCS, L- glutamine, and antibiotics (ThermoFisher, Waltham; ref. 73). A day before the experiment, the media were replaced with FluoroBrite Dulbecco's Modified Eagle Medium (DMEM) (ThermoFisher) to reduce background fluorescence (74). For organisms treated with local HL stress, following fumigation with H2DCFDA or PO1, illumination of 1,700 μmol photons m^{-2} s^{-1} was applied to a local leaf/area for 2 min using a light emitted diode (LED) fiber optic (Schott), as described previously (20, 23, 26, 37). Heat injury, following treatments with H2DCFDA or PO1 was applied for *D. discoideum* and mammalian cells using an open-flame-heated metal rod that touched the local injury area for 1 s (22). Hydrogen peroxide was applied as a 1 μL drop of 10 mM diluted in the buffer of the medium in which the organism was cultured. DPI (50 μM) or water was applied as a strip of 0.05% agarose (applied with a pipette tip along the center of the plate; Fig. 2A) for

P. patens, *C. reinhardtii*, and *D. discoideum*, or in the media for mammalian cells 5 or 10 min prior to the stress application (20).

Isolated Heart Studies. Mice used in this study were housed under pathogen-free conditions in animal care facilities and received humane care in compliance with the Guide for the Care and Use of Laboratory Animals (https://www.ncbi.nlm.nih.gov/books/NBK54050/; ref. 75). All experimental procedures were approved by the Institutional Animal Care and Use Committee of the University of Missouri (https://research.missouri.edu/acqa/acuc). C57BL/6 J mice were obtained from Jackson Laboratory (https://www.jax.org/) at 8 wk of age and used between the age of 9 and 10 wk of age. Mice were placed under anesthesia and hearts immediately collected (75). The hearts were rinsed in FluoroBrite DMEM (ThermoFisher). They were then incubated in Fluro Bright DMEM media containing 10% Fetal Bovine Serum, 15 mM 2-[4-(2-hydroxyethyl)piperazin-1-yl] ethanesulfonic acid (HEPES), 10 μM H_2DCFDA or 20 μM PO1 (Millipore-Sigma), and Penicillin–Streptomycin 10,000 units/mL (Gibco; ThermoFisher) for 2 h with gentle rocking in a CO_2 incubator (Binder C170; ThermoFisher); media were replaced twice during incubation, and a third time, just before imaging with the same media, but without H_2DCFDA or PO1. For DPI treatments, DPI (50 μM final concentration) was added to the incubation media 30 min prior to imaging. For catalase treatments, catalase (100 U/mL final concentration; Millipore-Sigma) was similarly added to the incubation. Isolated hearts were wounded or unwounded with an open-flame-heated rod (22) and immediately imaged.

ROS Imaging. All organisms, outside of mammalian cells and isolated hearts, were fumigated with 50 μM H_2DCFDA (Ex./Em. 480 nm/520 nm; Millipore-Sigma), or 20 μM Peroxy Orange 1 (PO1; Ex./Em. 540 nm/620 nm; Millipore-Sigma), in 0.05 M phosphate buffer pH 7.4 with 0.01% Silwet L-77. Fumigation was carried out for 30 min using nebulizers (20–24, 37, 38). For mammalian cells and isolated hearts 10 μM H_2DCFDA, or 20 μM PO1 (final concentrations) were applied to the medium for 30 min (cell cultures) or 2 h (isolated hearts). Following H_2DCFDA/PO1 fumigation/incubation, local stress/wounding was applied, and organisms/isolated hearts were imaged for live H_2O_2/ROS accumulation using the IVIS Lumina S5 platform (20–24, 37, 38, 76). To inhibit mammalian NOXs, APX115 (50 μM; Med Chem Express) and/or Setanaxib (50 μM; Med Chem Express), final concentrations, were added together with H_2DCFDA or PO1 to the growth media 30 min prior to stimulus application. To scavenge H_2O_2, catalase (100 U/mL final concentration; Millipore-Sigma) was fumigated together with PO1 or added to the media of H9c2 cells or isolated hearts 30 min prior to imaging. Acquired images were then analyzed according to refs. 20–24, 37 and 38. Empty agar plates were also fumigated with DCF (OxyBurst; 50 μM; ref. 19), treated with H_2O_2 and imaged as described above.

Protein Blot Analysis. Local and systemic cells of *C. reinhardtii* from treated or untreated plates, with or without DPI, 2 min or 30 min after a 2 min HL treatment, were collected and subjected to protein blot analysis with anti-sHSP17.1 as described previously (24, 25).

Proteomics Analysis. *Chlamydomonas* cells were grown on agar plates and subjected to HL stress as described above for 10 min. Local HS was applied by touching the agar surface 0.5 cm away from cells with a 100 °C heated 10-mm steel bar for 10 min (the temperature of the cells sampled next to the heated area was 37 °C measured with a FLIR camera as described in ref. 27). After 30 min, cells from the local and systemic areas (Fig. 3*A*) and cells from unstressed plates were scraped into Laemmli buffer X1, boiled, and centrifuged at 16,000 g for 10 min. The supernatant was precipitated with cold acetone. Ten micrograms of protein from each sample were then subjected to proteomics analysis as described in ref. 77. The database *C. reinhardtii* UP000006906 was used for searching. Differential abundance was determined using unpaired *t* tests. Post-analysis based on both MS level and a significance threshold of q-value < 0.05 and an absolute average log2 (fold change) > 0.58 were used to identify significant candidates (77).

Statistical Analysis. All experiments were repeated at least three times with at least three biological repeats. Box plots graphs are presented with mean as X ± SE; median is the line in the box and box borders are 25th and 75th percentiles; whiskers are the 1.5 interquartile range. The paired Student *t* test was conducted using Microsoft Excel (*$P < 0.05$; **$P < 0.01$; ***$P < 0.001$).

1. M. B. Miller, B. L. Bassler, Quorum sensing in bacteria. *Annu. Rev. Microbiol.* **55**, 165–199 (2001).
2. Q. Fan *et al.*, Structure and signal regulation mechanism of interspecies and interkingdom quorum sensing system receptors. *J. Agric. Food Chem.* **70**, 429–445 (2022).
3. M. Gambino, F. Cappitelli, Mini-review: Biofilm responses to oxidative stress. *Biofouling* **32**, 167–178 (2016).
4. K. U. Mahto, S. Kumari, S. Das, Unraveling the complex regulatory networks in biofilm formation in bacteria and relevance of biofilms in environmental remediation. *Crit. Rev. Biochem. Mol. Biol.* **57**, 305–332 (2022).
5. N. D. Holland, Early central nervous system evolution: An era of skin brains? *Nat. Rev. Neurosci.* **4**, 617–627 (2003).
6. S. V. Ovsepian, V. B. O'Leary, N. P. Vesselkin, "Chapter One - Evolutionary origins of chemical synapses" in *Vitamins and Hormones, Hormones and Synapse*, G. Litwack, Ed. (Academic Press, 2020), pp. 1–21.
7. A. S. O. Chávez, A. J. O'Neal, L. Santambrogio, M. Kotsyfakis, J. H. F. Pedra, Message in a vesicle – trans-kingdom intercommunication at the vector–host interface. *J. Cell Sci.* **132**, jcs224212 (2019).
8. Q. Zhou *et al.*, Extracellular vesicles: Their functions in plant–pathogen interactions. *Mol. Plant Pathol.* **23**, 760–771 (2022).
9. M. A. Marchionni, Neuregulin signaling in pieces–evolution of the gene family. *Cur. Pharm. Des.* **20**, 4856–4873 (2014).
10. J. Matkó, E. A. Tóth, Membrane nanotubes are ancient machinery for cell-to-cell communication and transport. Their interference with the immune system. *Biol. Futura* **72**, 25–36 (2021).
11. J. Ariazi *et al.*, Tunneling nanotubes and gap junctions–their role in long-range intercellular communication during development, health, and disease conditions. *Front. Mol. Neurosci.* **10**, 333 (2017).
12. Y. Combarnous, T. M. D. Nguyen, Cell communications among microorganisms, plants, and animals: Origin, evolution, and interplays. *Inter. J. Mol. Sci.* **21**, 8052 (2020).
13. J. Ghanam *et al.*, DNA in extracellular vesicles: From evolution to its current application in health and disease. *Cell Biosci.* **12**, 37 (2022).
14. M. Anfang, E. Shani, Transport mechanisms of plant hormones. *Curr. Opin. Plant Biol.* **63**, 102055 (2021).
15. C. Furumizu *et al.*, The sequenced genomes of nonflowering land plants reveal the innovative evolutionary history of peptide signaling. *Plant Cell* **33**, 2915–2934 (2021).
16. E. E. Farmer, Y.-Q. Gao, G. Lenzoni, J.-L. Wolfender, Q. Wu, Wound- and mechanostimulated electrical signals control hormone responses. *New Phytol.* **227**, 1037–1050 (2020).
17. Y. Fichman, R. Mittler, Integration of electric, calcium, reactive oxygen species and hydraulic signals during rapid systemic signaling in plants. *Plant J.* **107**, 7–20 (2021).
18. Q. Shao, Q. Gao, D. Lhamo, H. Zhang, S. Luan, Two glutamate- and pH-regulated Ca2+ channels are required for systemic wound signaling in Arabidopsis. *Sci. Signal.* **13**, eaba1453 (2020).
19. G. Miller *et al.*, The plant NADPH oxidase RBOHD mediates rapid systemic signaling in response to diverse stimuli. *Sci. Signal.* **2**, ra45 (2009).
20. Y. Fichman, G. Miller, R. Mittler, Whole-plant live imaging of reactive oxygen species. *Mol. Plant* **12**, 1203–1210 (2019).
21. Y. Fichman, S. I. Zandalinas, S. Peck, S. Luan, R. Mittler, HPCA1 is required for systemic reactive oxygen species and calcium cell-to-cell signaling and plant acclimation to stress. *Plant Cell* **34**, 4453–4471 (2022).
22. M. Szechyńska-Hebda *et al.*, Aboveground plant-to-plant electrical signaling mediates network acquired acclimation. *Plant Cell* **34**, 3047–3065 (2022).
23. Y. Fichman, R. J. Myers, D. G. Grant, R. Mittler, Plasmodesmata-localized proteins and ROS orchestrate light-induced rapid systemic signaling in Arabidopsis. *Sci. Signal.* **14**, eabf0322 (2021).
24. Y. Fichman *et al.*, Phytochrome B regulates reactive oxygen signaling during abiotic and biotic stress in plants. *New Phytol.* **237**, 1711–1727 (2023).
25. N. Suzuki *et al.*, Temporal-spatial interaction between reactive oxygen species and abscisic acid regulates rapid systemic acclimation in plants. *Plant Cell* **25**, 3553–3569 (2013).
26. S. I. Zandalinas, S. Sengupta, D. Burks, R. K. Azad, R. Mittler, Identification and characterization of a core set of ROS wave-associated transcripts involved in the systemic acquired acclimation response of Arabidopsis to excess light. *Plant J.* **98**, 126–141 (2019).
27. S. I. Zandalinas *et al.*, Systemic signaling during abiotic stress combination in plants. *Proc. Nat. Acad. Sci. U.S.A.* **117**, 13810–13820 (2020).
28. M. A. Inupakutika, S. Sengupta, A. R. Devireddy, R. K. Azad, R. Mittler, The evolution of reactive oxygen species metabolism. *J. Exp. Bot.* **67**, 5933–5943 (2016).
29. Y. J. Taverne *et al.*, Reactive oxygen species: Radical factors in the evolution of animal life. *BioEssays* **40**, 1700158 (2018).
30. E. Hörandl, D. Speijer, How oxygen gave rise to eukaryotic sex. *Proc. R. Soc. B* **285**, 20172706 (2018).

31. J. M. C. Gutteridge, B. Halliwell, Mini-Review: Oxidative stress, redox stress or redox success? *Biochem. Biophys. Res. Commun.* **502**, 183–186 (2018).
32. J. Jabłońska, D. S. Tawfik, The evolution of oxygen-utilizing enzymes suggests early biosphere oxygenation. *Nat. Ecol. Evol.* **5**, 442–448 (2021).
33. Y. Fichman, R. Mittler, Noninvasive live ROS imaging of whole plants grown in soil. *Trends Plant Sci.* **25**, 1052–1053 (2020).
34. Z. C. Liu *et al.*, Physicochemical processes in the indirect interaction between surface air plasma and deionized water. *J. Phys. D Appl. Phys.* **48**, 495201 (2015).
35. A. Ledo, E. Fernandes, A. Salvador, J. Laranjinha, R. M. Barbosa, In vivo hydrogen peroxide diffusivity in brain tissue supports volume signaling activity. *Redox Biol.* **50**, 102250 (2022).
36. A. Ø. Tjell, K. Almdal, Diffusion rate of hydrogen peroxide through water-swelled polyurethane membranes. *Sens. Bio-Sens. Res.* **21**, 35–39 (2018).
37. S. I. Zandalinas, Y. Fichman, R. Mittler, Vascular bundles mediate systemic reactive oxygen signaling during light stress. *Plant Cell* **32**, 3425–3435 (2020).
38. S. I. Zandalinas, R. Mittler, Vascular and nonvascular transmission of systemic reactive oxygen signals during wounding and heat stress. *Plant Physiol.* **186**, 1721–1733 (2021).
39. J. M. R. Fürst-Jansen, S. de Vries, J. de Vries, Evo-physio: On stress responses and the earliest land plants. *J. Exp. Bot.* **71**, 3254–3269 (2020).
40. C. M. Hansel, J. M. Diaz, Production of extracellular reactive oxygen species by marine biota. *Annu. Rev. Mar. Sci.* **13**, 177–200 (2021).
41. T. Kawahara, M. T. Quinn, J. D. Lambeth, Molecular evolution of the reactive oxygen-generating NADPH oxidase (Nox/Duox) family of enzymes. *BMC Evol. Biol.* **7**, 109 (2007).
42. B. Lardy *et al.*, NADPH oxidase homologs are required for normal cell differentiation and morphogenesis in *Dictyostelium discoideum*. *Biochim. Biophys. Acta* **1744**, 199–212 (2005).
43. J. Aguirre, J. D. Lambeth, Nox enzymes from fungus to fly to fish and what they tell us about Nox function in mammals. *Free Radic. Biol. Med.* **49**, 1342–1353 (2010).
44. C. Ortega-Villasante, S. Burén, Á. Barón-Sola, F. Martínez, L. E. Hernández, In vivo ROS and redox potential fluorescent detection in plants: Present approaches and future perspectives. *Methods* **109**, 92–104 (2016).
45. D. A. Lauffenburger, A. F. Horwitz, Cell migration: A Physically integrated molecular process. *Cell* **84**, 359–369 (1996).
46. H. Sies *et al.*, Defining roles of specific reactive oxygen species (ROS) in cell biology and physiology. *Nat. Rev. Mol. Cell Biol.* **23**, 499–515 (2022).
47. M. P. Murphy *et al.*, Guidelines for measuring reactive oxygen species and oxidative damage in cells and in vivo. *Nat. Metab.* **4**, 651–662 (2022).
48. N. Smirnoff, D. Arnaud, Hydrogen peroxide metabolism and functions in plants. *New Phytol.* **221**, 1197–1214 (2019).
49. H. Sies, D. P. Jones, Reactive oxygen species (ROS) as pleiotropic physiological signalling agents. *Nat. Rev. Mol. Cell Biol.* **21**, 363–383 (2020).
50. R. Mittler, S. I. Zandalinas, Y. Fichman, F. Van Breusegem, Reactive oxygen species signalling in plant stress responses. *Nat. Rev. Mol. Cell Biol.* **23**, 663–679 (2022).
51. M. Čáp, L. Váchová, Z. Palková, Reactive oxygen species in the signaling and adaptation of multicellular microbial communities. *Oxid. Med. Cell. Longev.* **2012**, e976753 (2012).
52. H. Zheng *et al.*, Redox metabolites signal polymicrobial biofilm development via the NapA oxidative stress cascade in Aspergillus. *Curr. Biol.* **25**, 29–37 (2015).
53. A. Sukenik, A. Kaplan, Cyanobacterial harmful algal blooms in aquatic ecosystems: A comprehensive outlook on current and emerging mitigation and control approaches. *Microorganisms* **9**, 1472 (2021).
54. F. J. Martínez-Navarro *et al.*, Hydrogen peroxide in neutrophil inflammation: Lesson from the zebrafish. *Dev. Comp. Immunol.* **105**, 103583 (2020).
55. H. Iwashita, E. Castillo, M. S. Messina, R. A. Swanson, C. J. Chang, A tandem activity-based sensing and labeling strategy enables imaging of transcellular hydrogen peroxide signaling. *Proc. Nat. Acad. Sci. U.S.A.* **118**, e2018513118 (2021).
56. P. Niethammer, C. Grabher, A. T. Look, T. J. Mitchison, A tissue-scale gradient of hydrogen peroxide mediates rapid wound detection in zebrafish. *Nature* **459**, 996–999 (2009).
57. A. V. Kuznetsov, S. Javadov, V. Saks, R. Margreiter, M. Grimm, Synchronism in mitochondrial ROS flashes, membrane depolarization and calcium sparks in human carcinoma cells. *Biochim. Biophys. Acta* **1858**, 418–431 (2017).
58. W. Chen *et al.*, Overexpressed UCP2 regulates mitochondrial flashes and reverses lipopolysaccharide-induced cardiomyocytes injury. *Am. J. Transl. Res.* **10**, 1347–1356 (2018).
59. H. Buvelot, V. Jaquet, K.-H. Krause, "Mammalian NADPH oxidases" in *NADPH Oxidases: Methods and Protocols, Methods in Molecular Biology*, U. G. Knaus, T. L. Leto, Eds. (Springer, 2019), pp. 17–36.
60. D. Liang, A salutary role of reactive oxygen species in intercellular tunnel-mediated communication. *Front. Cell Dev. Biol.* **6**, 2 (2018).
61. F. Xing *et al.*, The relationship of redox with hallmarks of cancer: The importance of homeostasis and context. *Front. Oncol.* **12**, 862743 (2022).
62. Z. Liao, D. Chua, N. S. Tan, Reactive oxygen species: A volatile driver of field cancerization and metastasis. *Mol. Cancer* **18**, 65 (2019).
63. H. Tsutsui, S. Kinugawa, S. Matsushima, Oxidative stress and heart failure. *Am. J. Physiol. Heart Circ. Physiol.* **301**, H2181–H2190 (2011).
64. S. Cadenas, ROS and redox signaling in myocardial ischemia-reperfusion injury and cardioprotection. *Free Radic. Biol. Med.* **117**, 76–89 (2018).
65. H. Bugger, K. Pfeil, Mitochondrial ROS in myocardial ischemia reperfusion and remodeling. *Biochim. Biophys. Acta* **1866**, 165768 (2020).
66. Y. Fichman, R. Mittler, A systemic whole-plant change in redox levels accompanies the rapid systemic response to wounding. *Plant Physiol.* **186**, 4–8 (2021).
67. D. P. Jones, H. Sies, The Redox Code. *Antioxid. Redox Signal.* **23**, 734–746 (2015).
68. T. Murashige, F. Skoog, A revised medium for rapid growth and bio assays with tobacco tissue cultures. *Physiol. Plant.* **15**, 473–497 (1962).
69. A. Gunadi *et al.*, Accelerating gametophytic growth in the model hornwort Anthoceros agrestis. *Appl. Plant Sci.* **10**, e11460 (2022).
70. D. J. Cove *et al.*, The moss Physcomitrella patens: A novel model system for plant development and genomic studies. *Cold Spring Harb. Protoc.* **2009**, pdb.emo115 (2009).
71. A. B. Hope, N. A. Walker, *The Physiology of Giant Algal Cells* (Cambridge University Press, 1975).
72. R. Froquet, E. Lelong, A. Marchetti, P. Cosson, *Dictyostelium discoideum*: A model host to measure bacterial virulence. *Nat. Protoc.* **4**, 25–30 (2009).
73. Y.-S. Sohn *et al.*, NAF-1 and mitoNEET are central to human breast cancer proliferation by maintaining mitochondrial homeostasis and promoting tumor growth. *Proc. Nat. Acad. Sci. U.S.A.* **110**, 14676–14681 (2013).
74. O. Karmi *et al.*, Interactions between mitoNEET and NAF-1 in cells. *PLoS One* **12**, e0175796 (2017).
75. O. Karmi *et al.*, The [2Fe-2S] protein CISD2 plays a key role in preventing iron accumulation in cardiomyocytes. *FEBS Lett.* **596**, 747–761 (2022).
76. Q. Zhu *et al.*, Combination of antioxidant enzyme overexpression and N-acetylcysteine treatment enhances the survival of bone marrow mesenchymal stromal cells in ischemic limb in mice with type 2 diabetes. *J. Am. Heart Assoc.* **10**, e023491 (2021).
77. S. I. Zandalinas *et al.*, Expression of a dominant-negative AtNEET-H89C protein disrupts iron-sulfur metabolism and iron homeostasis in Arabidopsis. *Plant J.* **101**, 1152–1169 (2020).
78. Y. Fichman, L. Rowland, M. J. Oliver, R. Mittler, ROS are evolutionary conserved cell-to-cell stress signals. *ProteomeXchange*. http://www.ebi.ac.uk/pride, PXD042594. Accessed 31 May 2023.